

$^{128,130,132,134}\text{La}$ in the axially symmetric rotor model

U. Datta Pramanik and S. Bhattacharya
Saha Institute of Nuclear Physics, Calcutta 700 064, India
 (Received 30 September 1994)

Recent experimental data on positive-parity yrast states, based on the $\pi h_{11/2} \otimes \nu h_{11/2}$ configuration, of odd-odd $^{128,130,132,134}\text{La}$ are compared in a systematic way with the energies and transition probabilities calculated within the framework of the two quasiparticle, axially symmetric core model. It is found that very good agreement is obtained in $^{128,130}\text{La}$ assuming prolate deformation. Influence of the neutron Fermi level on the level properties in these two nuclei has also been studied. In the case of $^{132,134}\text{La}$, this model seems to indicate that this positive-parity yrast band may have an oblate deformation.

PACS number(s): 21.60.Ev, 23.20.Gq, 23.20.Js, 27.60.+j

I. INTRODUCTION

The study of the deformed odd-odd nuclei provides much useful and interesting information on the interplay between the collective rotation and the single-particle motion of two nonidentical nucleons. In this respect odd-odd nuclei in the γ -soft $A \sim 130$ mass region have drawn much attention due to the fact that they allow one to investigate the competition between the relatively strong shape driving forces caused, on the one hand, by the neutron quasiparticle situated in the upper part of the $h_{11/2}$ orbital and, on the other hand, by the proton quasiparticle at the lower part of the same high- j shell, leading to triaxial equilibrium shapes [1,2]. As these γ -polarizing effects are strongly dependent on the configurations of the valence quasiparticles, coexistence of structures of different spectroscopic characters is also possible. It has also been known that triaxial deformation, dynamical or static, affects the signature dependence of various observables [3-6]. A change in γ deformation, for example, will manifest itself through a change in the signature splitting. Thus, in the case of odd- A nuclei in this region, a systematic analysis of the observed signature splitting (for the neutron orbitals in odd- N or for the proton orbitals in odd- Z systems) can be very useful in determining the cause behind such effects. The variation observed in the level properties in the $\Delta I = 1$ and $\Delta I = 2$ sequences built on the $h_{11/2}$ orbital in the neighboring odd- N and/or odd- Z nuclei is also very helpful in this respect. Such properties are easily obtainable from the measured intensity ratios of competing $M1$ and $E2$ transitions within the same band ($\Delta I = 1$ sequence) and $B(M1; I \rightarrow I - 1)/B(E2; I \rightarrow I - 2)$ ratios. Based on the above experimental signatures, predictions of shape coexistence in the odd- A nuclei in this mass region had been made by several workers [7-14] for the $Z \sim 57$ and $N \geq 74$ nuclei. Such detailed studies in the case of odd-odd nuclei are difficult both experimentally and theoretically due to the complexity of their excited states. In the $A \sim 130$ region, such experimental investigations have just been initiated. Very recently, experimental signatures for shape coexistence in ^{134}Pr has been reported

by Petrache *et al.* [15]. A systematic analysis of the observed rotational bands in doubly odd nuclei in this region, using a shell model configuration mixing approach, has been carried out by Rizzutto *et al.* [16]. This analysis points to the possibility of observing a transition from a prolate to an oblate shape as the neutron number changes from 75 to 79. These authors [16] predict an oblate deformation in the case of ^{138}Pr .

In recent years, extensive experimental evidence for the existence of distinct band structures in odd-odd lanthanum nuclei have been obtained. It has created an opportunity for testing the predictions of different theoretical models on the level properties of these nuclei. The work of Rizzutto *et al.* [16] also contains a detailed calculation of the excitation energies of the states in odd-odd La nuclei. While this manuscript was under preparation we came across a study by Tajima [17], on the role of triaxiality and residual interaction in the $A \sim 130$. Though this paper mainly deals with the level properties of ^{124}Cs , it also contains a brief report of such studies on La isotopes. However, the results do not appear to be very encouraging. The section which refers to the La nuclei in this paper is also rather brief. Furthermore, none of these studies [16,17] provide electromagnetic transition properties of the calculated levels. In this paper we report the results of a systematic investigation carried out by us on the level properties of the yrast band based on the $\pi h_{11/2} \otimes \nu h_{11/2}$ configuration in $^{128,130,132,134}\text{La}$ nuclei within the framework of a two-quasiparticle, axial-rotor model. Godfrey *et al.* [18] have referred to a similar calculation by Semmes, but we have not so far come across, in the literature, any such studies for this entire set of odd-odd La nuclei using the same model. Furthermore, in view of the recent avalanche of experimental data on high-spin states in these nuclei, it is felt that an investigation using this simple model may be very useful to get some insight into the intricacies of their structures. It is of particular importance to verify the conjecture of the existence of triaxiality and shape coexistence in these nuclei.

The nuclei $^{128,130}\text{La}$ have been studied [18,19] exten-

sively experimentally. The salient features of these experimental studies are the observations of two distinct bands based on the $\pi h_{11/2} \otimes \nu h_{11/2}$ and $\pi h_{11/2} \otimes \nu g_{7/2}$ configurations. It has also been noted that there exists a close similarity between the band structures found in ^{128}La and ^{130}La . A few theoretical calculations within the cranked shell model and total Routhian surface (TRS) model have also been carried out [18,19] to predict the equilibrium values of the deformation parameters and to see the effect of the triaxiality parameter γ on the level energies. For higher-mass La nuclei, viz., $^{132,134}\text{La}$, such detailed experimental data for high-spin band members are still lacking. Heavy-ion reaction data giving some information on the band structures based on the $\pi h_{11/2} \otimes \nu h_{11/2}$ configuration in these La nuclei have been reported recently by Oliveira *et al.* [20,21]. Additional information on ^{134}La is also available from $(\alpha, 3n\gamma)$ reaction experiments [22,23]. Though these experiments have established bands up to 14^+ in both these isotopes, detailed electromagnetic transition properties are not yet available. Another band has been observed [20] in ^{132}La , and this has been tentatively assigned a $\pi \frac{3}{2} [422] \otimes \nu h_{11/2}$ configuration. No such negative-parity band has been reported in ^{134}La . In $^{128,130}\text{La}$ the observed signature splitting, in the band based on the $\pi h_{11/2} \otimes \nu h_{11/2}$ configuration, is about 40 keV [19], whereas the same is observed [20,21] to be 25 keV for ^{132}La and ~ 50 keV for ^{134}La . A comparison of the experimental branching ratios in $^{128,130}\text{La}$ with those available for $^{132,134}\text{La}$ indicates a significant change in the decay pattern. In the latter cases transitions connecting $I \rightarrow I - 1$ states are much stronger than the $I \rightarrow I - 2$ transitions for higher-spin states ($I \geq 11$). Furthermore, as far as the present experimental data indicate, the $\pi h_{11/2} \otimes \nu h_{11/2}$ band in $^{132,134}\text{La}$ does not mix with the other sidebands. So far, no theoretical attempt has been made to explain these facts.

II. MODEL

The present model is described in detail elsewhere [24–27], and only the salient features are mentioned here for the sake of completeness. As is well known, it is based on the assumption that the nuclei under consideration are axially symmetric and have reflection symmetry with respect to a plane perpendicular to its symmetry axis. The calculations of energies and wavefunctions are carried out within a framework wherein motions of an unpaired odd proton and odd neutron moving in Nilsson's deformed orbits are coupled to the rotational motion through Coriolis interaction. The total Hamiltonian of such a system can be written as

$$H = H_{\text{intrinsic}} + H_{\text{rot}} , \quad (1)$$

where

$$\begin{aligned} H_{\text{intrinsic}} &= H_{\text{av}} + H_{\text{pair}} + H_{\text{int}} \\ &\text{(neglecting the long-range } H_{\text{vibr}} \text{ term)} \\ &= H_{\text{Nils}(p)} + H_{\text{Nils}(n)} + H_{\text{pair}(p)} + H_{\text{pair}(n)} \\ &\quad + H_{\text{int}} . \end{aligned} \quad (2)$$

The rotational part of the Hamiltonian can be written more explicitly as

$$H_{\text{rot}} = \frac{\hbar^2}{2\mathcal{J}}(I^2 - I_3^2) + H_{\text{cor}} + H_{\text{ppc}} + H_{\text{irrot}} , \quad (3)$$

$$H_{\text{cor}} = -\frac{\hbar^2}{2\mathcal{J}}(I^+ j^- + I^- j^+) , \quad (4a)$$

$$H_{\text{ppc}} = -\frac{\hbar^2}{2\mathcal{J}}(j_p^+ j_n^- + j_p^- j_n^+) , \quad (4b)$$

$$H_{\text{irrot}} = \frac{\hbar^2}{2\mathcal{J}}[(j_p^2 - j_{pz}^2) + (j_n^2 - j_{nz}^2)] . \quad (4c)$$

\mathcal{J} is the moment of inertia with respect to the rotation axis. I^\pm , j_p^\pm , j_n^\pm , and j_n^\pm are the usual shifting operator. The set of basis eigenvectors are written in the form

$$\begin{aligned} |IMK\alpha\rangle &= \left[\frac{2I+1}{16\pi^2(1+\delta_{K0})} \right]^{1/2} [D_{M,K}^I |K\alpha\rangle \\ &\quad + (-)^{I+K} D_{M,-K}^I |K\alpha\rangle] , \end{aligned} \quad (5)$$

where R_i is the operator representing rotation around the second intrinsic axis and α characterizes the configuration of the odd proton and odd neutron such that

$$(H_{\text{av}} + H_{\text{pair}})|K\alpha\rangle = (\epsilon_p + \epsilon_n)|K\alpha\rangle . \quad (6)$$

ϵ_p and ϵ_n are the quasiparticle proton and neutron energies of the respective quasiparticle states. K is the projection of the total angular momentum onto the symmetry axis and coincides with the projection of the total particle angular momentum j in the case of an axially symmetric rotor. If Ω_p and Ω_n are the projections on the symmetry axis of the single-particle angular momenta j_p and j_n , respectively, then on account of the symmetry of the average field, K can be $\Omega_p + \Omega_n$ or $\Omega_p - \Omega_n$, with the constraint that $K \geq 0$. The n - p residual interaction H_{int} splits the energy of these Gallagher-Moszkowski doublets. In this work this interaction has been considered to be of diagonal nature having the form [26]

$$(H_{\text{int}})_{kk'} = -4G\langle \Sigma_p \rangle \langle \Sigma_n \rangle \delta_{kk'} , \quad (7)$$

where G is a constant. The expectation values $\langle \Sigma_p \rangle$ and $\langle \Sigma_n \rangle$ of the intrinsic spin projections of the protons and the neutrons, respectively, are calculated from Nilsson wave functions. This simplest approximation schematically includes the splitting of the $K = |\Omega_p| \pm |\Omega_n|$ doublets.

In our calculation we have incorporated the concept of a variable moment of inertia (VMI) to describe the energy levels of the core. This has been done in analogy with the VMI model and its two particle extension [26] by adding an ‘‘elastic energy’’ term $\frac{1}{2}C(\mathcal{J} - \mathcal{J}_0)^2$ to the Hamiltonian and applying the variational principle to the diagonal energies of the unperturbed rotational states. The usual pairing correction factor has been included in calculating single-particle matrix elements (occurring in the energy diagonalization and the calculation of electromagnetic transition probability) in this basis. Diagonalization of the total Hamiltonian matrix for each value

of the angular momentum I gives the theoretical energy values for all the bands built on the two-quasiparticle configuration present in the basis set of eigenfunctions. The final wave functions are thus linear combinations of (5).

The wave functions obtained have been used to calculate detailed electromagnetic transition probabilities, branching ratios, multipole mixing ratios, etc., and the approach is similar to one adopted by Reich, Helmer, and Greenwood [24] and Popli *et al.* [26]. Only collective and single-particle transitions have been considered, i.e., transitions in which both particles change states have been ignored. In the present calculation the mixing ratio (δ^2) has been defined to be the ratio of total $E2$ by total $M1$ transition probability. To understand the coupling of various angular momenta, the wave functions $|IMK\rangle$ have been transformed into a basis where R and J , the quantum numbers corresponding to the core angular momentum and the total particle angular momentum, respectively, are the constants of motion. The R and J distributions have then been calculated for different I states.

III. CHOICE OF PARAMETERS

This calculation involves a large number of parameters. In the absence of any constraints, these could be varied artificially to fit the data, but that would not be physically meaningful. The main objective of the present work is to attempt an understanding, in a systematic way, of the band structure in odd-odd La on the basis of a simple application of Nilsson model with Coriolis coupling. We have, therefore, tried to reduce the number of independent variables to a minimum by choosing either a global set of parameters for this region or using the relevant experimental data to extract out the necessary parameters. Furthermore, a full-scale variation of these independent parameters has been held to a minimum. There are six Nilsson neutron states and six Nilsson proton states which contribute to this band structure. The calculation has been performed within this full basis. The μ, κ parameters of the deformed modified oscillator potential are the standard values used in this mass region for $N = 5$ shell. The pairing gaps (Δ_p and Δ_n) and the Fermi levels (λ_p and λ_n) are then deduced by solving the inverse gap equation. The quadrupole deformation parameter β for each nuclei is obtained from the experimental β_2 values of the respective core [28]. The VMI parameter \mathcal{J}_{0K} , which is the minimum moment of inertia for an unperturbed rotational state $|IMK\rangle$, has been defined for odd-A case [29] to be

$$\mathcal{J}_{0K} = \mathcal{J}_{IK} \quad (I = j_0),$$

where j_0 is the angular momentum of the spherical shell model state to which the state degenerates at zero deformation. Since it is difficult to make such realistic definition for \mathcal{J}_{0K} 's in the odd-odd case, we have set these to be equal to zero, as has been done by earlier worker [26]. No artificial attenuation of the Coriolis or recoil term is

needed. The strength parameter G of the n - p interaction has been varied from $G = 0.0$ to 0.8 MeV. It is found that $G = 0.4$ MeV gives a better fit to the energies and transition properties in $^{128,130}\text{La}$ (comparison has been made for these two cases as extensive experimental data are available) and this value has subsequently been kept fixed for the other nuclei. The VMI parameter C has been varied from case to case to get a better fit to the band structures.

The calculation of the $M1$ transition probabilities has been carried out by using the following values for the g factors: $g_R = Z/A$, $(g_l)_p = 1$, $(g_l)_n = 0$, $(g_s)_p = 5.585$, and $(g_s)_n = -3.826$. The intrinsic quadrupole moment which appears in the expression for the rotational $E2$ transition has been calculated from the respective experimental $B(E2; 2_1^+ \rightarrow 0_1^+)$ values of the core [28]. Calculations of $E2$ transition rates have been carried out with different sets of combination for effective charges of neutrons (0.5 and 1.0) and protons (1.0 and 1.5). Since the major contribution is from the collective part and changes in the effective charges affect the particle part, only minor variations have been noticed in the final calculated results for the $E2$ transition rates within this band. Results for the $(e_p)_{\text{eff}} = (e_n)_{\text{eff}} = 1.0$ are, therefore, presented in this paper. In calculating the transition probabilities between two states, the corresponding experimental energy values have been used.

It is essential to mention at this point that we have considered only states from 8^+ and above in the fitting procedure, and the parameters thus obtained have then been utilized to calculate the properties of the lower-spin states ($I \leq 8$). The reasons for doing this are the following. In $^{132,134}\text{La}$, the bands have been established experimentally [20,21] from 8^+ and above and no proper identification of the other lower-spin members has been made. For ^{128}La and ^{130}La , though the band structures have been identified from 4^+ and 6^+ , respectively [18,19], attempts to get a fit of the energy levels relative to these states result in rather larger deviation in energy values between theory and experiment at high-spin states ($I \geq 12$). Furthermore, the agreement between theoretical and experimental transition probabilities also

TABLE I. Parameters used in the calculation. In all the calculations $\mu_p = 0.5$, $\mu_n = 0.35$, and $\kappa_p = \kappa_n = 0.0637$.

Parameters	^{128}La	^{130}La	^{132}La	^{134}La
Core	^{126}Ba	^{128}Ba	^{130}Ba	^{132}Ba
β	0.27	0.23	0.22	0.18
λ_p (MeV)	45.55	45.35	45.12	44.94
			44.97 ^a	44.80 ^a
Δ_p (MeV)	1.01	0.98	0.96	1.00
			1.00 ^a	1.08 ^a
λ_n (MeV)	49.51	49.38	49.63	49.29
			49.07 ^a	48.92 ^a
Δ_n (MeV)	0.80	0.73	0.68	0.69
			0.89 ^a	0.76 ^a
C ($\times 10^7$ keV ³)	1.50	2.20	0.85	1.65
$Q_0(b)$	4.37	3.70	3.60	2.94

^aValues used in the calculation with oblate deformation.

becomes worse.

The parameters used in the present calculation are listed in Table I. It is to be noted here that in the present calculation the only adjustable parameters are C and G , the latter one again being fixed after some initial variations, as mentioned earlier. It will be revealed from the following discussions that even with this minimum adjustment good overall agreements have been obtained.

IV. RESULTS AND DISCUSSION

The results will be presented in three subsections, viz., (i) calculation in $^{128-134}\text{La}$ with a prolate deformation, (ii) dependence of the energy and the transition probabilities in $^{128,130}\text{La}$ on the choice of λ_n and G in the above-mentioned case of prolate deformation, and (iii) calculation in $^{132,134}\text{La}$ with an oblate deformation.

A. Prolate deformation in $^{128-134}\text{La}$

In Fig. 1 we have shown the calculated and experimental energies for $^{128-134}\text{La}$. The spectra are plotted relative to the 8^+ state. In this figure we have also shown the positions of the 4^+-7^+ spin states in ^{128}La and $6^+, 7^+$ states in $^{130-134}\text{La}$. It can be seen from the figure that there is a good overall agreement between the experimental data and the theoretical predictions. The calculation is able to reproduce satisfactorily the general trend in the change of the experimental energy levels by using only one adjustable parameter, i.e., C . It can, however, be seen that the calculated states below 8^+ are rather squeezed in energy compared to the experimental ones. It is also found that the predicted bandhead spin for ^{128}La is 5^+ , while it is 6^+ for $^{130-134}\text{La}$. The calculated 4^+ state is found to lie above the 8^+ state in $^{130-134}\text{La}$. The 5^+ state is above the 6^+ state in $^{130,132}\text{La}$, while it moves

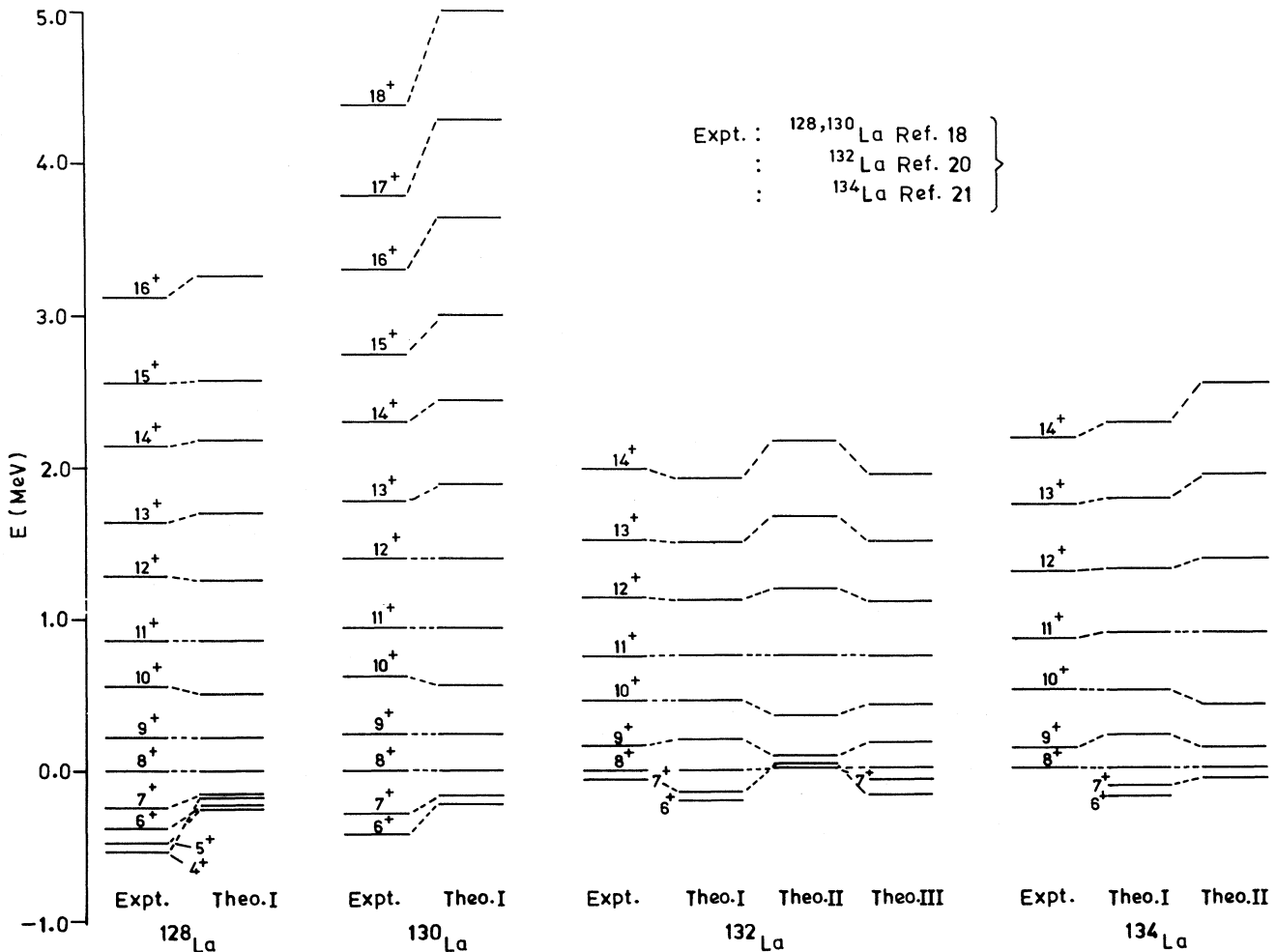


FIG. 1. Comparison of (Expt.) experimental positive-parity levels based on the $\pi h_{11/2} \otimes \nu h_{11/2}$ configuration in $^{128-134}\text{La}$: (Theo. I) relevant portion of the theoretical spectrum assuming a prolate deformation and (Theo. II) relevant portion of the theoretical spectrum in $^{132,134}\text{La}$ assuming an oblate deformation without any change in the parameters from the prolate case. Theo. III in the case of ^{132}La indicates the theoretical spectrum obtained with an oblate deformation, but with some changed parameters (see text for details). The excitation energies are shown relative to the 8^+ state.

above the 7^+ in ^{134}La . In the case of ^{130}La , the theoretical prediction is in agreement with the experimental findings of Godfrey *et al.* [18]. Rotational states based on $\pi h_{11/2} \otimes \nu h_{11/2}$ configuration have been established conclusively from 6^+ and above. Several weak transitions have been found depopulating this yrast 6^+ level. The experimentally observed lower-spin states, in that case, are most probably not members of the same band and may have different origins. It may be mentioned here that a good agreement with the intraband γ -transition probability data has been obtained in the case of $^{128,130}\text{La}$. The above facts lend support to our approach of using this model (with restricted n - p interaction) in these nuclei. We will discuss later about the bandhead spins in $^{132,134}\text{La}$.

A probable reason for the disagreement in the energy values at the low-spin region in $^{128,130}\text{La}$ may be due to the fact that the rotational Hamiltonian H_{rot} may not necessarily be the dominant part of the total Hamiltonian for these low-spin states in which the core rotations are small. Thus the inclusion of a realistic residual two-body interaction and extending the configuration space may have a larger effect on the properties of the calculated low-spin states. For the high-spin states, the contribution of such a two-body interaction has been shown to be small [25].

It can also be seen from Fig. 2 that the experimental

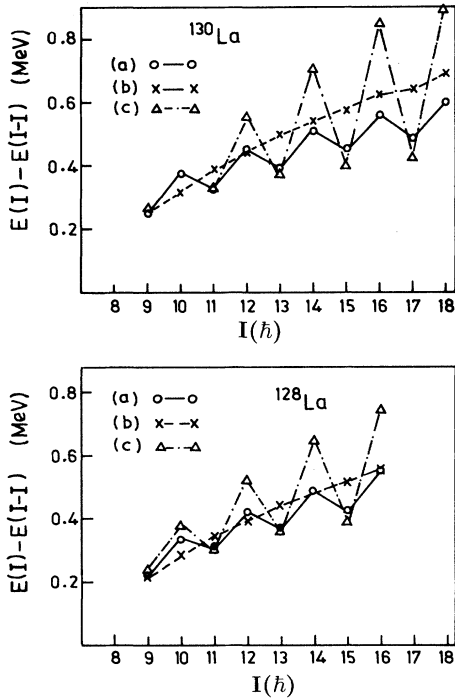


FIG. 2. Comparison of (a) the experimental staggering of the yrast band based on $\pi h_{11/2} \otimes \nu h_{11/2}$ configuration in $^{128,130}\text{La}$ with (b) the theoretical values obtained with prolate deformation, $G = 0.4$ MeV and λ_n , as obtained from the solution of the inverse gap equation, and (c) the theoretical values obtained by a proper choice of λ_n so as to reproduce the experimental staggering. Experimental data are taken from Ref. [18].

energy staggerings are not correctly reproduced. This feature has been observed in earlier calculations also [16,17] involving triaxiality and thus is not a failure of the axial symmetric model only. One reason for such behavior may be somewhat wrong choice of the neutron Fermi level, which, as mentioned earlier, has been obtained from the solution of the inverse gap equation. We have, therefore, tried to look into the effect of variation of neutron Fermi level on the energy spectra and the transition properties in $^{128,130}\text{La}$.

B. Effect of λ_n and G

We will now discuss the results of our study on the sensitivity of the calculated level properties on the choice of λ_n and G . In the case of a prolate deformation, the neutron Fermi surface, obtained through the solution of the inverse gap equation, is near to the $\frac{7}{2}[523]$ orbital in ^{128}La and moves close to the $\frac{9}{2}[514]$ orbital in $^{132,134}\text{La}$. The proton Fermi level, on the other hand, is near the $\frac{1}{2}[550]$ and $\frac{3}{2}[541]$ orbitals. The favored signature component ($\alpha = -\frac{1}{2}$) of the $h_{11/2}$ proton orbital is coupled to both signature components ($\alpha = \pm\frac{1}{2}$) of the neutron orbitals giving rise to $\Delta I = 1$ bands. The high- Ω neutron states involved have small signature splitting. Furthermore, the bands, arising from the coupling of the unfavored signature component of the proton orbital with the neutron orbitals, lie high above the yrast line as a result of large signature splitting of the proton orbital and are not observed. Thus relatively small energy splitting or its absence between the two signature components is expected in the $\Delta I = 1$ band with the present position of the λ_n near the high- Ω neutron orbitals. In the case of $^{128,130}\text{La}$ we have, therefore, varied λ_n near the low- Ω orbitals so as to first reproduce the experimentally observed staggering in energy. It has been found that the best fit is obtained with the neutron Fermi level near the $\frac{3}{2}[541]$ orbital ($\lambda_n = 46.8$ MeV for ^{128}La and 46.85 MeV for ^{130}La). In Fig. 2 we have shown these results by plotting $[E(I) - E(I-1)]$ vs I wherein we have also included the results with λ_n as obtained from the solution of the inverse gap equation. In both the cases G has been taken to be 0.4 MeV. In Fig. 3 the experimental $B(M1; I \rightarrow I-1)/B(E2; I \rightarrow I-2)$ ratios have been plotted against I along with the calculated ones. Figure 4 shows similar plots for the branching ratios. In both these figures, calculated values for (a) $G = 0.0, 0.4,$ and 0.8 MeV (with λ_n as obtained from inverse gap equation) and (b) $G = 0.4$ MeV and $\lambda_n = 46.8$ MeV for ^{128}La (46.85 MeV for ^{130}La) are included to show the effect of (i) n - p interactions and (ii) the position of Fermi level in the transition properties. It is apparent from Figs. 2–4 that though by proper choice of λ_n we have been able to reproduce the staggering in energy, the transition probability data are not reproduced (both in magnitude and in trends), particularly at low spins. Figures 3 and 4 also demonstrate how this simple spin-spin interaction affects the results, particularly for the transitions between the higher members of the bands. The agreement between the theory and experiment is extremely good for $G = 0.4$

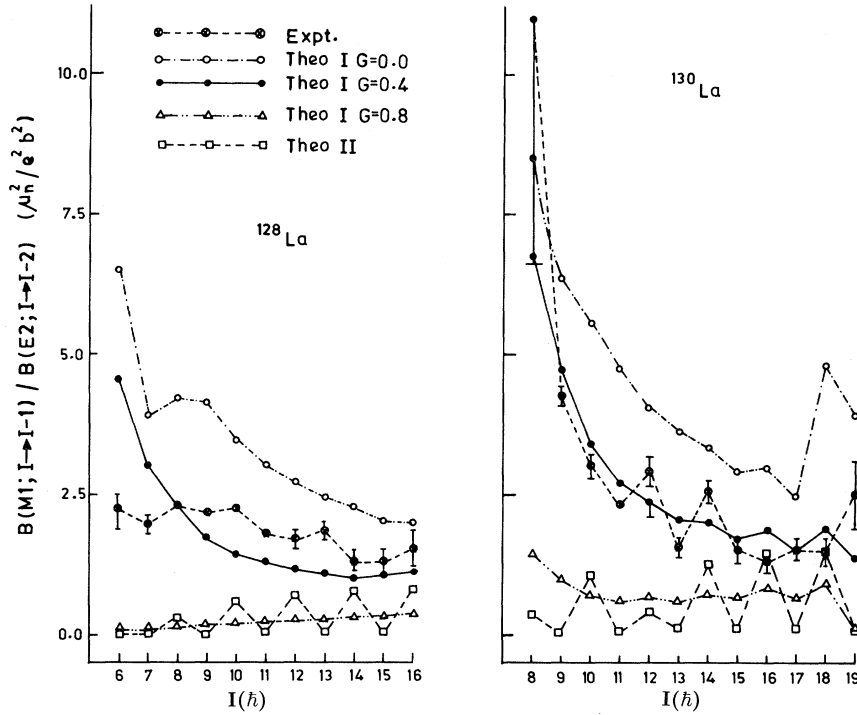


FIG. 3. Experimental and theoretical $B(M1; I \rightarrow I - 1) / B(E2; I \rightarrow I - 2)$ ratios in ^{128}La and ^{130}La are plotted against spin. The theoretical values (Theor. I) obtained with $G = 0.0, 0.4,$ and 0.8 MeV and λ_n from the solution of the inverse gap equation are also shown. Theor. II are the theoretical results obtained with λ_n so chosen as to reproduce the experimental staggering in energy. Experimental data are taken from Ref. [18].

MeV for these two nuclei. It is therefore strongly felt that it is not necessary to introduce triaxiality to explain the experimental results in $^{128,130}\text{La}$. At this point it is worthwhile to mention the work of Tajima [17] which attempts to study the effect of triaxiality in this region. However, a meaningful comparison between the results obtained by us using axially symmetric deformation and those of Tajima cannot be made because the electromagnetic properties for the La isotopes are not given in the later work.

Before discussing the results of the calculation of electromagnetic properties in more detail, it may be interesting, at this point, to note some general features of the wave function of the states. The orbitals $\pi \frac{1}{2}[550], \pi \frac{3}{2}[541]$

and $\nu \frac{7}{2}[523], \nu \frac{9}{2}[514]$ mainly influence the structure of the states in these nuclei for prolate deformation. In ^{128}La the K structures remain more or less similar from 4^+ onwards, as far as the major contributions are concerned. The configuration of the states with spin 8^+ and above is, however, not a simple one. They are of mixed configurations, with the $\pi \frac{1}{2}[550] \otimes \nu \frac{7}{2}[523]$ ($K = 3,4$) and $\pi \frac{3}{2}[541] \otimes \nu \frac{7}{2}[523]$ ($K = 2,5$) being the most dominant ones. In ^{130}La the states are highly mixed in character, compared to other La nuclei studied here. Even in the low-spin region, $\pi \frac{1}{2}[550] \otimes \nu \frac{9}{2}[514]$ ($K = 4,5$) and $\pi \frac{3}{2}[541] \otimes \nu \frac{9}{2}[514]$ ($K = 3,6$) states have relatively larger contributions in the wave functions. This may be one of the reasons for the relatively high value

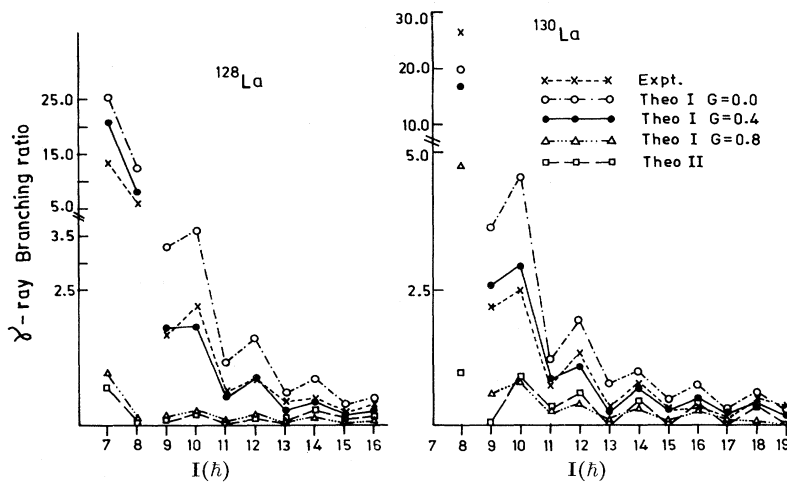


FIG. 4. Experimental and theoretical γ -ray branching ratios in $^{128,130}\text{La}$ are plotted against spin. Other details are the same as in Fig. 3.

of the experimental $B(M1)/B(E2)$ ratios in ^{130}La compared to those in ^{128}La . Another point worth mentioning here is that in our calculation the contributions from the $\pi_{\frac{5}{2}}[532] \otimes \nu_{\frac{9}{2}}[514]$ ($K = 7$), $\pi_{\frac{1}{2}}[550] \otimes \nu_{\frac{5}{2}}[532]$ ($K = 3$) and $\pi_{\frac{3}{2}}[541] \otimes \nu_{\frac{5}{2}}[532]$ configurations are found to be insignificant. This is in contradiction to the results of Rizzutto *et al.* [16]. According to them, these orbitals are important and responsible for energy staggering. An agreement with the energy staggering data does not guarantee that the wave functions thus obtained truly represent the states concerned. The correct nature of the wave functions can only be ascertained through a comparison of the calculated electromagnetic transition properties with the observed ones. In view of the fact that no theoretical values for transition probabilities have been reported by Rizzutto *et al.*, it is, therefore, difficult to judge the true importance of these states.

In ^{132}La , the $\pi_{\frac{1}{2}}[550] \otimes \nu_{\frac{9}{2}}[514]$ and $\pi_{\frac{3}{2}}[541] \otimes \nu_{\frac{9}{2}}[514]$ configurations account for about 86% of the strength in $I = 6$, slowly reducing to 66% in $I = 9$ and to 55% in $I = 14$. Again, in ^{134}La , these states are slightly more mixed in nature compared to ^{132}La . These features are expected to have their reflections in the transition probability data. In Tables II and III we have compared the results of our calculation for the transition probabilities with the experimental results for ^{128}La and ^{130}La , while the same information for ^{132}La and ^{134}La is given in Tables IV and V. It can be seen from Tables II and III that there is an excellent agreement with the experimen-

tal results in the case of $^{128,130}\text{La}$. Owing to a lack of transition probability data, the comparisons with experiment become less meaningful for $^{132,134}\text{La}$ nuclei. The situation is relatively more difficult for ^{132}La where the experimental branching ratios cannot be properly evaluated within all the spin states as two important transitions (*viz.*, 293 and 455 keV) appear twice in the level scheme. So a detailed comparison is not possible, but the results of this part of the calculation are not in good agreement with the general trend of the transition probability data for these two isotopes (Tables IV and V). This is, however, expected because (as mentioned earlier in the Introduction) a significant change in the decay pattern is observed experimentally in $^{132,134}\text{La}$ compared to that in $^{128,130}\text{La}$. Since the main motivation behind the present calculation is to get an understanding of the level properties in these nuclei in a systematic way, no abrupt variation in the parameters has been made to fit the properties of the individual isotopes. Therefore no major changes in the calculated level properties are expected with the present set of parameters, as one moves from $A = 128$ to 134.

A plausible reason for such changes in the level properties may be that the triaxiality plays an important role in the higher-mass odd-odd La nuclei. However, the systematics of the experimental excitation energies and the results of the Cranking Shell Model calculations [18,20,21] are not in favor of such an increase in the triaxiality parameter for these nuclei compared to $^{128,130}\text{La}$. A

TABLE II. Calculated and experimental decay modes of the $\pi h_{11/2} \otimes \nu h_{11/2}$ yrast band in ^{128}La .

I_i^π	I_f^π	Theoretical $T(E2) + T(M1)$ $\times 10^{10}$ (sec^{-1})	Branching ratio		Theor. ^a		$B(M1)/B(E2)$ $\mu_n^2/(eb)^2$	
			Expt. ^b	Theor. ^a	$B(E2)$ (eb) ²	$B(M1)$ μ_n^2	Expt. ^b	Theor. ^a
6 ⁺	5 ⁺	0.59	96.1	97.8	0.35	0.30	2.23	3.95
	4 ⁺	0.013	3.9	2.2	0.07			
7 ⁺	6 ⁺	2.54	93.1	95.4	0.36	0.54	1.94	4.55
	5 ⁺	0.12	6.9	4.6	0.12			
8 ⁺	7 ⁺	11.16	85.4	88.9	0.37	0.47	2.29	3.02
	6 ⁺	1.40	14.6	11.1	0.15			
9 ⁺	8 ⁺	8.23	63.4	64.6	0.37	0.41	2.17	2.25
	7 ⁺	4.51	36.6	35.4	0.18			
10 ⁺	9 ⁺	25.87	69.1	64.8	0.35	0.36	2.24	1.71
	8 ⁺	14.06	30.9	35.2	0.21			
11 ⁺	10 ⁺	16.81	40.1	36.1	0.34	0.34	1.81	1.43
	9 ⁺	29.79	59.9	63.9	0.24			
12 ⁺	11 ⁺	48.09	47.9	44.0	0.31	0.33	1.67	1.27
	10 ⁺	61.09	52.1	56.0	0.26			
13 ⁺	12 ⁺	30.61	30.6	22.6	0.29	0.32	1.84	1.14
	11 ⁺	104.72	69.4	77.4	0.28			
14 ⁺	13 ⁺	79.26	33.3	31.7	0.27	0.34	1.31	1.12
	12 ⁺	170.98	66.7	68.3	0.30			
15 ⁺	14 ⁺	50.13	18.8	16.2	0.25	0.32	1.32	1.00
	13 ⁺	258.85	81.2	83.8	0.31			
16 ⁺	15 ⁺	116.74	28.6	24.2	0.24	0.35	1.56	1.07
	14 ⁺	365.70	71.4	75.8	0.33			

^aCalculation with prolate deformation.

^bReference [18].

TABLE III. Calculated and experimental decay modes of the $\pi h_{11/2} \otimes \nu h_{11/2}$ yrast band in ^{130}La .

I_i^π	I_f^π	Theoretical $T(E2) + T(M1)$ $\times 10^{10}$ (sec^{-1})	Branching ratio		Theor. ^a		$B(M1)/B(E2)$ $\mu_n^2/(eb)^2$	
			Expt. ^b	Theor. ^a	$B(E2)$ (eb) ²	$B(M1)$ μ_n^2	Expt. ^b	Theor. ^a
8 ⁺	7 ⁺	23.06	96.5	94.6	0.26	0.57	11.02	6.75
	6 ⁺	1.30	3.5	5.3	0.08			
9 ⁺	8 ⁺	13.73	69.2	72.1	0.27	0.51	4.23	4.64
	7 ⁺	5.31	30.8	27.9	0.11			
10 ⁺	9 ⁺	42.87	71.7	74.6	0.26	0.44	3.09	3.46
	8 ⁺	14.63	28.3	25.4	0.13			
11 ⁺	10 ⁺	25.96	40.5	45.7	0.25	0.41	2.30	2.72
	9 ⁺	30.88	59.5	54.3	0.15			
12 ⁺	11 ⁺	66.66	57.6	54.0	0.23	0.39	2.93	2.34
	10 ⁺	56.72	42.4	46.0	0.17			
13 ⁺	12 ⁺	42.59	24.4	31.2	0.22	0.38	1.54	2.04
	11 ⁺	93.83	75.6	68.8	0.18			
14 ⁺	13 ⁺	100.40	44.8	40.8	0.20	0.39	2.56	1.98
	12 ⁺	145.74	55.2	59.2	0.20			
15 ⁺	14 ⁺	60.46	19.3	22.8	0.19	0.36	1.50	1.72
	13 ⁺	204.88	80.7	77.2	0.21			
16 ⁺	15 ⁺	141.27	24.7	33.4	0.17	0.41	1.33	1.85
	14 ⁺	282.36	75.3	66.6	0.22			
17 ⁺	16 ⁺	74.14	16.4	17.2	0.16	0.34	1.51	1.50
	15 ⁺	356.98	83.6	82.8	0.23			
18 ⁺	17 ⁺	172.07	23.7	28.8	0.15	0.42	1.51	1.79
	16 ⁺	424.69	76.3	71.2	0.24			
19 ⁺	18 ⁺	82.68	14.8	13.9	0.14	0.32	2.52	1.32
	17 ⁺	476.48	85.2	86.1	0.24			

^aCalculation with prolate deformation.^bReference [18].

more realistic n - p interaction may also bring a significant change in the calculated values. The third alternative is that these bands in $^{132,134}\text{La}$ may be of a different collective shape (viz., oblate shape), whereas the similar bands in $^{128,130}\text{La}$ are prolate in nature. We have studied this

aspect of the problem in detail and this will be discussed in the next subsection.

Before proceeding further it may be mentioned at this point that ^{134}La is weakly deformed ($\beta = 0.18$) compared to $^{128-132}\text{La}$ ($\beta = 0.27-0.22$). Therefore the valid-

TABLE IV. Calculated and experimental decay modes of the $\pi h_{11/2} \otimes \nu h_{11/2}$ yrast band in ^{132}La .

I_i^π	I_f^π	Branching ratio			Theoretical $B(M1)/B(E2)$ $\mu_n^2/(eb)^2$			Theoretical mixing ratio δ^2			
		Expt. ^a	I ^b	II ^c	III ^d	I ^b	II ^c	III ^d	I ^b	II ^c	III ^d
9 ⁺	8 ⁺		85.1	99.4	99.6	0.48	157.1	29.5	0.22	0.001	0.001
	7 ⁺		14.9	0.6	0.4						
10 ⁺	9 ⁺		60.8	99.4	99.7	0.60	77.4	23.0	0.39	0.007	0.006
	8 ⁺		39.2	0.6	0.3						
11 ⁺	10 ⁺		31.0	94.8	87.4	0.69	34.1	13.2	0.25	0.010	0.009
	9 ⁺		69.0	5.2	12.6						
12 ⁺	11 ⁺	90.2	37.4	92.3	84.8	0.80	20.5	9.5	0.30	0.020	0.016
	10 ⁺	9.8	62.6	7.7	15.2						
13 ⁺	12 ⁺	92.7	24.0	81.1	68.1	0.90	14.6	7.7	0.21	0.018	0.013
	11 ⁺	7.3	76.0	18.9	31.9						
14 ⁺	13 ⁺		28.0	79.0	68.1	0.99	11.4	6.5	0.22	0.023	0.016
	12 ⁺		72.0	21.0	32.0						

^aReference [21].^bCalculation with prolate deformation.^cCalculation with oblate deformation with the same set of parameters as in the prolate case.^dCalculation with oblate deformation with changed parameters (see text).

TABLE V. Calculated and experimental decay modes of the $\pi h_{11/2} \otimes \nu h_{11/2}$ yrast band in ¹³⁴La.

I_i^π	I_f^π	Branching ratio			Theoretical $B(M1)/B(E2)$ $\mu_n^2/(eb)^2$		Theoretical mixing ratio δ^2	
		Expt. ^a	Theor.		I ^b	II ^c	I ^b	II ^c
			I ^b	II ^c				
10 ⁺	9 ⁺		81.5	99.6	1.87	141.7	0.19	0.007
	8 ⁺		18.5	0.4				
11 ⁺	10 ⁺	60.3	32.4	94.6	1.47	60.9	0.14	0.008
	9 ⁺	39.7	67.6	5.4				
12 ⁺	11 ⁺	91.8	40.3	93.0	1.30	30.2	0.21	0.018
	10 ⁺	8.2	59.7	7.0				
13 ⁺	12 ⁺	60.8	25.4	84.3	1.23	22.6	0.18	0.016
	11 ⁺	39.2	74.6	15.7				
14 ⁺	13 ⁺	85.5	27.4	81.5	1.22	17.0	0.21	0.019
	12 ⁺	14.5	72.6	18.5				

^aReferences [20,21].^bCalculation with prolate deformation.^cCalculation with oblate deformation with the same set of parameters as in the prolate case.

ity of the particle rotor model (PRM), which inherently assumes a core with good rotational behavior, may be questioned in such cases. This point has been addressed earlier by Stephens [30] who noted good agreement between the PRM predictions and experimental results for weakly deformed odd-*A* nuclei in the La-Ce region. Later detailed comparative studies of several odd-*A* nuclei in the well-deformed region with those in transitional region have been carried out by other workers [29,31] and also by us [32] within the framework of the PRM. It has been observed that the PRM, which incorporates both pairing and variable moment of inertia (VMI) formalisms, works reasonably well in weakly deformed systems in various regions of the periodic table. The inclusion of the VMI formalism approach provides an additional flexibility in the model in the sense that a more realistic description of the core behavior can be achieved even in the case of a weakly deformed system. The application of the PRM for the odd-odd cases has been so far quite limited, and no such detailed comparative study has been carried out. However, observations made earlier in the case of an odd-*A* system and successes achieved in the description of odd-odd Ag isotopes ($\beta = 0.12$) within the PRM formalism [26,33] render support to the idea of applying this model to the case of ¹³⁴La.

C. Comparison between prolate and oblate shape predictions in ^{132,134}La

We have calculated the level properties of ^{132,134}La assuming an oblate deformation (with $\beta = -0.23$ and -0.186 , respectively) for their equilibrium shapes. The values of λ_n , Δ_p , λ_n , and Δ_n as obtained through a solution of the inverse gap equation are given in Table I. The energy spectra are shown in Fig. 1 and the transition probability data are listed in Tables IV and V. It can be seen from the Nilsson diagrams that the $h_{11/2}$ levels are

symmetric with respect to zero deformation, while the neutron and proton Fermi levels are situated at the very top and bottom, respectively, of the above subshell. This results in a unique shell filling of the last neutron and proton. Thus the $\pi \frac{1}{2}[550]$, $\frac{3}{2}[541]$ and $\nu \frac{7}{2}[523]$, $\frac{9}{2}[514]$ are the dominant orbitals for the prolate deformation, but in the case of oblate deformation the $\pi \frac{11}{2}[505]$, $\frac{9}{2}[514]$, $\nu \frac{1}{2}[550]$, $\frac{3}{2}[541]$, and $\frac{5}{2}[532]$ orbitals play the significant role. This also results in an extension of the dimension of the basis states considered in *K* space. In the prolate case the maximum values of *K* chosen is 8 (as $K > 8$ have very little influence on the calculated results), while in the case of oblate deformation $K \geq 8$ are found to have an appreciable influence on the calculated results for $I \geq 8$ spin states. The theoretical energy spectra show good overall agreement for both positive and negative values of the β , though the states calculated with positive β show somewhat better agreement. It has been found that an adjustment of the parameters (*G* and/or attenuation coefficients) can produce equally good agreement for a negative β , and the result of one such fitting for ¹³²La is shown in Fig. 1 (“Theor. III”). However, our main objective is to see how far the transition probability values are affected by considering an oblate shape instead of a prolate shape (keeping every other parameter unchanged). We will, therefore, first concentrate on that part of the calculation in which parameters are same except for those which are effected by the change of sign of β . At the end we will discuss the necessity of changing the parameters in the case of ¹³²La.

The calculation with oblate deformation indicates a bandhead spin of 7⁺ for ^{132,134}La. In the case of ¹³²La, the calculated 7⁺ and 8⁺ states are degenerate in energy. In their work on ¹³²La, Oliveira *et al.* [20] have primarily assigned a spin parity of 8⁺ to the bandhead, but at the same time they have also proposed a state with a spin parity of 7⁺, which is consistent with the systematics

in the $N = 75$ isotones, viz., ^{134}Pr and ^{136}Pm . This 7^+ state is connected by a 67-keV $M1$ transition with the 8^+ state, but no experimental signature is available to decide on the parentage of this state. The calculated lifetime for this $8^+ \rightarrow 7^+$ transition (assuming $E_\gamma = 67$ keV) in the case of prolate and oblate deformations are 0.23 and 0.04 nsec, respectively. The calculated mixing ratio (δ^2) for this transition is 0.15 for the prolate case and < 0.001 for the oblate deformation. A measurement of these quantities will, therefore, be interesting. In the case of ^{134}La , no such 7^+ state has been definitely identified experimentally so far. Several states have been reported [21–23] which are connected to the yrast 8^+ state, but for them definite spin parities have not been assigned yet. Attempts should, therefore, be made to identify such states in ^{134}La .

It can be seen from Table V (in the case of ^{134}La) that the calculations not only correctly reproduce the experimental systematics, but also are in very good agreement with the experimental branching ratios. It would be interesting to discuss the case of deexcitation of the 10^+ yrast state in this case. Experimentally, no transition has been found connecting this state to the 8^+ state. Using the experimental value [21,22] for the relative intensity (~ 83) of the 381.6-keV γ ray ($10^+ \rightarrow 9^+$) and the theoretically predicted branching ratio of the 10^+ state from Table V, the relative intensity of the unobserved 527-keV γ ray ($10^+ \rightarrow 8^+$) can be calculated. This comes out to be 19.0 for a prolate deformation and 0.3 for an oblate deformation. Nonobservance of this transition further supports the oblate shape. The ^{134}La data show a staggering in the branching ratios which are not reflected in the present calculation. In the absence of any data on the $B(M1)/B(E2)$ ratio, it is not possible to extend the discussion any further.

In the case of ^{132}La , the experimental and theoretical branching ratios for the oblate shape are in very good agreement for the 12^+ and 13^+ states (Table IV). The situation is, however, not so favorable for the transitions involving other states in view of the following facts. As mentioned earlier, the 293- and 455-keV transitions appear twice in the level scheme. The intensity of one of the components of the 455-keV γ ray ($14^+ \rightarrow 13^+$) can be estimated by assuming the experimental intensity (~ 2) of the 841-keV γ ray ($14^+ \rightarrow 12^+$) and the theoretical branching ratio for the γ rays originating from the 14^+ state. Similarly, the one part of the intensity of the 293-keV γ ray ($11^+ \rightarrow 10^+$) can be estimated from the experimental intensity (5.6) of the 588-keV γ ray ($11^+ \rightarrow 9^+$) and the theoretical branching ratio of the 11^+ state. Taking the total intensity of the 293-keV γ ray to be 90.7 from the experiment [20], one can estimate the intensity of the second 293-keV transition depopulating the 10^+ state. This in turn can provide the intensity of the other 455-keV ($10^+ \rightarrow 8^+$) transition. The total intensity of the 455-keV γ ray can then be compared with the experimental one (7.2 ± 0.7) [20]. Following the above procedures and using the branching ratios given in Table IV, total intensity for the 455-keV γ ray comes out to be 57.6 for the prolate deformation. In the case of oblate deformation, the estimated intensities of the sin-

gle 455-keV ($14^+ \rightarrow 13^+$) and the 293-keV ($11^+ \rightarrow 10^+$) transitions are found to be very large compared to the experimentally observed total intensities. It is, therefore, clear that although the branching ratios of the 12^+ and 13^+ states are in apparent agreement with the values obtained in the oblate case, the other calculated branching ratios do not support the corresponding experimental results. We have, therefore, recalculated the level properties of ^{132}La by adjusting the parameters slightly for the oblate core, and the best fit with the energies is obtained with the following changed parameters (others being kept fixed): $G = 0.1$ MeV and $\lambda_p = 45.8$ MeV. It is seen from Fig. 1 (“Theor. III”) that the energy values of the states are quite well reproduced. The very good agreement obtained in energy for the yrast 7^+ state is encouraging. The calculated lifetime for the 67-keV transition connecting 8^+ to 7^+ is 0.05 nsec and the mixing ratio is 0.002 for these set of parameters. The electromagnetic transition properties are given in Table IV (“Theor. III”). The branching ratios obtained in this case for the γ transitions originating from the 12^+ and 13^+ states differ to some extent from the experimental ones, but the total intensity of the 455-keV transition, calculated in the manner described above, is found to be 5.4, close to the experimental value. The intensities of two 293-keV transitions also seem to be consistent with the overall decay pattern. How far these predictions are true can only be judged from a more accurate measurement of the intensities of the γ rays. It has also been noted [20] that there is a very close similarity between the $\pi h_{11/2} \otimes \nu h_{11/2}$ bands observed in the isotones ^{132}La , ^{134}Pr , and ^{136}Pm . So these results can also be compared with the data in ^{134}Pr and ^{136}Pm . We are also calculating the level properties of these isotones, and the results will be reported soon. Nevertheless, we feel that all the above considerations strongly suggest that $\pi h_{11/2} \otimes \nu h_{11/2}$ bands in $^{132,134}\text{La}$ have an oblate deformation.

V. CONCLUSION

From the present calculation on the properties of the yrast states (based on the $\pi h_{11/2} \otimes \nu h_{11/2}$ configuration) in $^{128,130,132,134}\text{La}$, within an axially symmetric rotor model the following conclusions may be arrived at.

(a) The calculation is able to reproduce satisfactorily the general trend in the change of the experimental energy levels from $A = 128$ to 134 by using only one adjustable parameter, viz., C .

(b) The electromagnetic transition properties in $^{128,130}\text{La}$ are very well reproduced with prolate deformation.

(c) The experimental staggering in $^{128,130}\text{La}$ is not correctly reproduced. This can be reproduced by a suitable choice of the neutron Fermi level. In that case agreement with the transition probability data (in magnitudes and in trends) is not obtained in the low-spin region. But some agreement in the high-spin states has been obtained. In trying to ascertain the cause behind this, the first obvious choice would be to see the role of triaxiality. But such a study carried out very recently in this region

and particularly in $^{124,126,128,130,132}\text{La}$ does not give very encouraging results. In view of this and the overall good agreement obtained in $^{128,130}\text{La}$ with the axially symmetric rotor model, it is felt that the triaxiality may not play a significant role in these two nuclei. It would be interesting to see whether a more realistic residual interaction can produce simultaneously the experimental staggering and the electromagnetic properties of these yrast levels. The role of triaxiality can be judged better by analyzing the level properties of the nonyrast states rather than that of the yrast states.

(d) In $^{132,134}\text{La}$ equally good agreement to the energy spectra is obtained for both positive and negative values of the deformation. Furthermore, in view of the limited transition probability data in these nuclei, it becomes rather difficult to arrive at a definite conclusion regarding their equilibrium shapes. However, the calculated transition probabilities in the present work favors an oblate deformation in $^{132,134}\text{La}$, though it supports a prolate nature for the band based on similar configura-

tion in $^{128,130}\text{La}$. The neutron and proton Fermi levels in these nuclei are situated at the top and the bottom of the $h_{11/2}$ state. The last proton, therefore, occupies the low- Ω orbitals, while the last neutron occupies the high- Ω orbitals of the same high- j state. Considering this unique shell filling of the last proton and the neutron and the corresponding shape-polarizing effects associated with them, it is felt that there is a distinct possibility of obtaining such a change in shape with the addition of neutrons. Several predictions on the transition rates $B(M1; I \rightarrow I - 1)/B(E2; I \rightarrow I - 2)$ ratios and mixing ratios $[\delta^2 = T(E2; I \rightarrow I - 1)/T(M1; I \rightarrow I - 1)]$ have been made. A measurement of these quantities is, therefore, necessary to decide on the above aspect of the equilibrium shape.

The authors are grateful to Professor S. Sen for many helpful discussions and for a critical review of the manuscript.

-
- [1] G. A. Leander, S. Frauendorf, and F. R. May, in *Proceedings of the Conference on High Angular Momentum Properties of Nuclei*, edited by N. R. Johnson (Harwood Academic, New York, 1983), p. 218.
- [2] Y. S. Chen, S. Frauendorf, and G. A. Leander, *Phys. Rev. C* **28**, 2437 (1988).
- [3] R. Bengtsson, H. Frisk, F. R. May, and J. A. Pinston, *Nucl. Phys.* **A415**, 189 (1984).
- [4] S. Frauendorf and F. R. May, *Phys. Lett.* **125B**, 245 (1983).
- [5] I. Hamamoto and B. R. Mottelson, *Phys. Lett.* **132B**, 7 (1983).
- [6] A. Ikeda, *Nucl. Phys.* **A439**, 317 (1973).
- [7] J. R. Leigh, K. Nakai, K. H. Maier, F. Puhlhofer, F. S. Stephens, and R. M. Diamond, *Nucl. Phys.* **A213**, 1 (1973).
- [8] J. Meyer-Ter-Vehn, *Nucl. Phys.* **A249**, 111 (1975).
- [9] J. Meyer-Ter-Vehn, *Nucl. Phys.* **A249**, 141 (1975).
- [10] J. Gizon, A. Gizon, R. M. Diamond, and F. S. Stephens, *J. Phys. G* **4** L171 (1978).
- [11] M. Müller-Veggian, G. Gono, R. M. Lieder, A. Neskakis, and C. Mayer-Böricke, *Nucl. Phys.* **A304**, 1 (1978).
- [12] M. Kortelahti, A. Pakkanen, M. Piiparinen, T. Komppa, and R. Komu, *Nucl. Phys.* **A376** 1 (1982).
- [13] L. Hildingsson, C. W. Beausang, D. B. Fossan, R. Ma, E. S. Paul, W. F. Piel, Jr., and N. Xu, *Phys. Rev. C* **39**, 471 (1989).
- [14] D. Bazzacco, S. Lunardi, G. Nardelli, M. De Poli, and G. de Angelis, *Z. Phys. A* **335**, 363 (1990).
- [15] C. M. Petrache, G. de Angelis, D. Bucurescu, M. Ivascu, D. Bazzacco, and S. Lunardi, *Z. Phys. A* **344**, 227 (1992).
- [16] M. A. Rizzutto, E. W. Cybulska, L. G. R. Emediato, N. H. Medina, R. V. Ribas, K. Hara, and C. L. Lima, *Nucl. Phys.* **A569**, 547 (1994).
- [17] N. Tajima, *Nucl. Phys.* **A572**, 365 (1994).
- [18] M. J. Godfrey, Y. He, I. Jenkins, A. Kirwan, P. J. Nolan, D. J. Thornely, S. M. Mullins, and R. Wadsorth, *J. Phys. G* **15**, 487 (1989).
- [19] E. S. Paul, C. W. Beausang, D. B. Fossan, R. Ma, W. F. Piel, Jr., N. Xu, and L. Hildingsson, *Phys. Rev. C* **36**, 1853 (1987).
- [20] J. R. B. Oliveira, L. G. R. Emediato, M. A. Rizzutto, R. V. Ribas, W. A. Seale, M. N. Rao, N. H. Medina, S. Botelho, and E. W. Cybulska, *Phys. Rev. C* **39**, 2250 (1989).
- [21] J. R. B. Oliveira, L. G. R. Emediato, E. W. Cybulska, R. V. Ribas, W. A. Seale, M. N. Rao, N. H. Medina, M. A. Rizzutto, S. Botelho, and C. L. Lima, *Phys. Rev. C* **45**, 2740 (1992).
- [22] U. Datta Pramanik, A. Mukherjee, M. Saha, A. Goswami, P. Basu, M. L. Chatterjee, B. Dasmahapatra, S. Sen, and S. Bhattacharya, *Proc. Nucl. Phys. Symp.* **36B**, 60 (1993).
- [23] T. Morek, H. Beuscher, B. Bochev, T. Kutsarova, R. M. Lieder, M. Müller-Veggian, and A. Neskakis, *Nucl. Phys.* **A433**, 159 (1985).
- [24] C. W. Reich, R. G. Helmer, and R. C. Greenwood, *Nucl. Phys.* **A168**, 487 (1971).
- [25] C. Flaum and D. Cline, *Phys. Rev. C* **14**, 1224 (1976).
- [26] Rakesh Popli, F. A. Rickey, L. E. Samuelson, and P. C. Simms, *Phys. Rev. C* **23**, 1085 (1981).
- [27] A. K. Jain, J. Kvasil, R. K. Sheline, and R. W. Hoff, *Phys. Rev. C* **40**, 432 (1989).
- [28] S. Raman, C. H. Malarkey, W. T. Milner, C. W. Nestor, Jr., and P. H. Stelson, *At. Data Nucl. Data Tables* **36**, 1 (1987).
- [29] H. A. Smith, Jr. and F. A. Rickey, *Phys. Rev. C* **14**, 1946 (1976).
- [30] F. S. Stephens, *Rev. Mod. Phys.* **47**, 43 (1975).
- [31] Rakesh Popli, J. A. Grau, S. I. Popik, L. E. Samuelson, and P. C. Simms, *Phys. Rev. C* **20**, 1350 (1979); Rakesh Popli, F. A. Rickey, and P. C. Simms, *ibid.* **22**, 1121 (1980); P. C. Simms, F. A. Rickey, and R. K. Popli, *Nucl. Phys.* **A347**, 205 (1980).

- [32] A. Goswami, S. Bhattacharya, M. Saha, and S. Sen, Phys. Rev. C **37**, 370 (1988); M. Saha, S. Bhattacharya, A. Goswami, and S. Sen, Z. Phys. A **332**, 383 (1989); M. Saha, A. Goswami, S. Bhattacharya, and S. Sen, Phys. Rev. C **42**, 1386 (1990).
- [33] A. Goswami, M. (Saha) Sarkar, U. Datta Pramanik, P. Banerjee, P. Basu, P. Bhattacharya, S. Bhattacharya, M. L. Chatterjee, S. Sen, and B. Dasmahapatra (unpublished).